MEGA JOURNAL OF CASE REPORTS

OPEN ACCESS

Research Article

Compiled Date: May 10, 2024

Coupled Effect of the Presence of Plaque and Carotid Web for the Assessment of hemodynamic parameters in a Patient Carotid Artery: A CFD Study

Kaveh Moghadasi*, Mergen H. Ghayesh*, Eric Hu and Jiawen Li

School of Electrical and Mechanical Engineering, University of Adelaide, Adelaide, South Australia 5005, Australia

***Corresponding authors**: Kaveh Moghadasi, School of Electrical and Mechanical Engineering, University of Adelaide, Adelaide, South Australia 5005, Australia

Mergen H. Ghayesh, School of Electrical and Mechanical Engineering, University of Adelaide, Adelaide, South Australia 5005, Australia

Abstract

Cerebrovascular accident remains as a prevailing contributor to mortality in contemporary times. The coexistence of vulnerable plaque and carotid web within the carotid artery represents a significant indicator for determining the likelihood of thrombus formation, leading to stroke and prolonged disabilities. In this paper computational fluid dynamics (CFD) as a computational method has been employed to examine the effects of carotid artery hemodynamic characteristics and to predict the likelihood of plaque rupture inside the artery. In the developed model, blood flow was assumed to be non-Newtonian, turbulent, and pulsatile. The simulated results (from the model) revealed that the hemodynamic characteristics of the carotid artery were notably impacted by the geometric attributes of plaques and carotid web, alongside flow conditions. A significant disturbed flow patterns were observed in the sinus region of the artery. Relatively diminished wall shear stress in the region downstream of the plaque dilation at the carotid bifurcation was also observed, which was a known contributor to atherosclerotic plaque development.

Keywords: Carotid; Plaque; Carotid web; Computational fluid dynamics

Introduction and Background

Stroke stands as a substantial contributor to both disability and mortality [1,2]. Approximately 20 % of all strokes are caused by carotid artery stenosis and rupture of an atherosclerosis plaque in the artery [3]. Carotid artery performs the vital task of efficiently supplying oxygenated blood to the brain. It is located bilaterally in the neck, comprising three sections: Common Carotid Artery (CCA), Internal Carotid Artery (ICA), and External Carotid Artery (ECA). The complexity of carotid arterial system necessitates performing biomechanical computational analysis utilising patient-specific data. This approach aims to

either mitigate more severe clinical events or minimise the incidence of unnecessary surgeries, or to provide a comprehensive understanding of hemodynamic parameters on the plaque regions prone to rupture and emergency treatment of the patient. Accordingly, hemodynamic simulation studies using Computational Fluid Dynamics (CFD) has been extensively utilised to enhance comprehension of the functional, diagnostic, and therapeutic implications of blood flow within the arterial system. Development of atherosclerosis is the main cause of carotid artery disease. Atherosclerosis is a condition characterised by the occlusion of major arteries within the human circulatory system, resulting in diminished or inadequate blood flow to tissues. Arteriosclerotic plaques commonly form near the carotid artery bifurcation, where the CCA branches into the Internal and External Carotid Arteries (ICA and ECA) [4]. Moreover, carotid sinus, owing to possessing values of Wall Shear Stress (WSS) less than 1.5 pa, is known for atherosclerosis prone region [5]. Carotid web is described a linear shape and spur-like intraluminal projection observed along the proximal ICA posterior region through angiography [6]. Histologically, the defining characteristic of a carotid web is fibrous intimal thickening [7]. Unlike conventional atherosclerotic disease, the carotid web is recognised as a manifestation of Fibromuscular Dysplasia (FMD) [8]. The carotid web is recognised as an infrequent contributor to ischemic strokes, notably recurrent in younger adult patients. Its occurrence near the proximal aspect of the ICA is believed to accelerate accumulation of atherosclerotic plaque and clot formation. Within the carotid arteries, complex flow patterns are considered to exert a significant influence on localised hemodynamic stresses [9,10]. Elevated peak stresses within the fibrous cap of carotid plaques are associated with an increased risk of rupture. Biomechanical models are employed to evaluate stresses within these plaques, typically employing CFD techniques to analyse patient-specific artery.

Literature Review on CFD Analyses of Carotid Artery

Computational Fluid Dynamic (CFD) analyses are increasingly employed to explore hemodynamic parameters and their changes under pathological conditions, crucial signs for diagnosing cerebrovascular and cardiovascular diseases. CFD simulation has demonstrated its reliability in modelling arterial blood flow. CFD not only offers a three-dimensional visualisation of pressure and velocity fields but also provides the distribution of wall shear stress and pressure gradient, which is challenging to acquire through direct measurements. In the following, some findings of other researchers are discussed. Kumar et al. [11] conducted a comparative analysis of different models of blood viscosity, including Power Law, Carreau and Newtonian to assess their impact on hemodynamic parameters employing CFD analysis. Low Wall Shear Stress (WSS) regions leading to flow reversals and in areas comprising stenosis with reduced diameter, the Newtonian model tends to overestimate hemodynamic parameters and lacks accuracy in predicting outcomes. In contrast, the Carreau model offers improved approximations at critical sites. In another study, Lee et al. [12] assessed the quantitative influence of various methods to incorporate the influence of blood viscosity on WSS levels through CFD analysis. The Wall Shear Stress (WSS) values during the end-diastolic phase, as determined by Newtonian models, were roughly thirty percent less compared to those obtained using a non-Newtonian model. This research highlights the necessity of integrating non-Newtonian behaviour of the blood flow, specific blood viscosity of the patients, the geometry of the artery, and precise inlet flow conditions into blood flow simulations for accurately WSS calculation across arterial segments. Li et al. [13] conducted a three-dimensional CFD analysis of the carotid artery, modelling rigid walls and considering blood flow as non-Newtonian, laminar, and pulsatile transient. The study revealed that the blood flow in the proximity of the outer sidewalls of the carotid sinus (positioned at ICA) and the ECA exhibited notably reduced velocity and dynamic pressures, accompanied by an intensified velocity angle. The carotid bifurcation exhibited a notable rise in WSS. Kanokjaruvijit et al. [14] carried out a three dimensional analysis of a carotid artery employed from Movahed [15] model. The blood flow considered incompressible,

non- Newtonian, and laminar. The highest values of WSS were identified at the locations with minimum flow area, characterised by elevated velocities. At 60% stenosis, there was a notable increase in WSS peak in the symmetric case. Sousa et al. [16] used 2D cross-sectional and longitudinal images for the carotid artery reconstruction. Blood flow modelled isotropic, incompressible, homogeneous, Newtonian viscous fluid Pulsatile transient flow. Remarkable agreement noted between ultrasound imaging data and results from computational simulations. Previous studies have primarily concentrated on assessing hemodynamic parameters in carotid artery atherosclerosis plaques. However, none of the published works considered combined effect of both atherosclerosis and carotid web, and how they influence WSS and blood velocity within the artery.

The objective of the current study is to identify the hemodynamic parameters that influence atherosclerotic regions by utilising a three-dimensional computational model to analyse fluid dynamics in a diseased carotid artery with the existence of a carotid web. The blood is considered incompressible, non-Newtonian, turbulent and pulsatile. Hence, twofold aims are considered; First, WSS magnitudes are computed at pivotal locations to assess the potential for plaque development and rupture within the arterial system. Secondly, the velocity profiles at different time steps are assessed to observe the velocity variation at carotid bifurcated region and carotid sinus.

Method

Geometry reconstruction

The carotid artery geometry utilised in this study was derived from Ref. [17], reconstructed via MATLAB 2021b [18] and ANSYS 2023R1 [19] based on data from a patient without any specific cardiovascular disease [20]. The carotid web model features a web length of 4.5 mm and an acute angle of 73.2°. To identify atherosclerotic plaques within the carotid geometry, a severe condition of the patient artery was simulated, incorporating a number of plaques at three distinct locations to the geometry of the model in [17], determined to have the highest likelihood of plaque presence based on prior research. Carotid stenosis measurement is generally measured by criterion from the European Carotid Surgery Trial (ESCT) and the North American Symptomatic Carotid Endarterectomy Trial (NASCET) [21]. According to these trials and based on surgical indications, the moderate stenosis is considered 50% to 69% of the lumen. Hence, in the present study, two plaques situated at the carotid apex and carotid bulb are modelled accordingly, while the plaque proximal to the ECA (before bifurcation) is simulated with a lesser severity (<50%). **Figure 1** shows the geometry of carotid artery including both plaques at different locations and carotid web posterior to carotid bulb. The model was discretised using tetrahedral elements in ANSYS Fluent 2023R1. The fluid domain comprised 624,587 elements, with a mesh skewness of approximately 0.5.

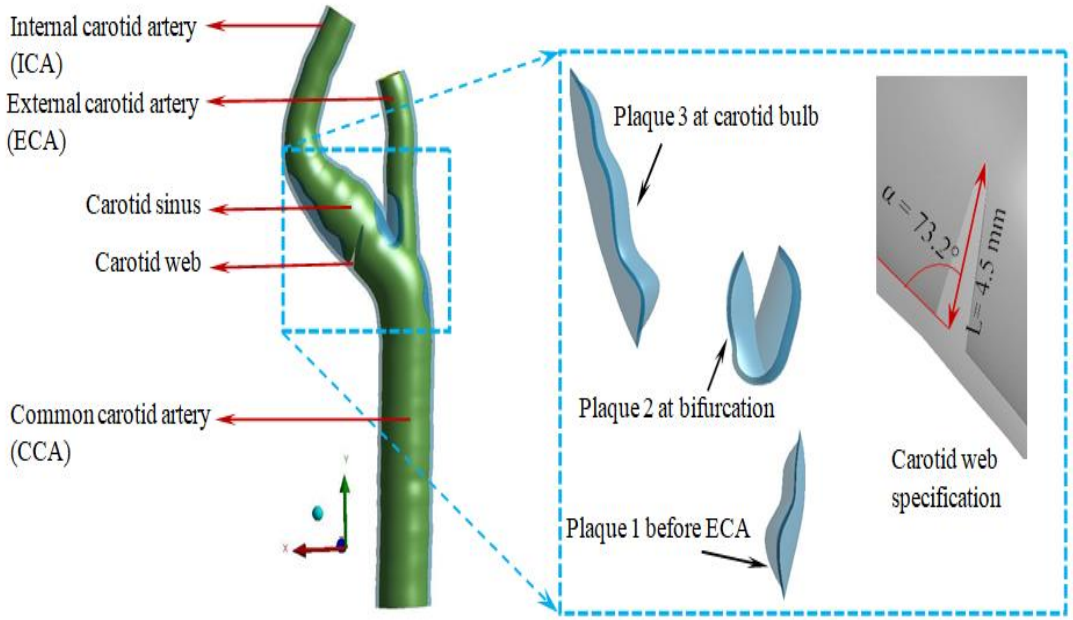

Figure 1: Carotid artery model, showing location of plaques and carotid web. The simpler version of this diagram (with no plaques) has previously been reported in **[17]**.

Blood model

Blood flow is modelled as a non-Newtonian, pulsatile, turbulent and incompressible, characterised by a density ρf = 1060 kg/m3. To facilitate the comprehensive analysis of fluid dynamics within the arterial system, the solved governing equations for mass and momentum conservation are **[22,23]**:

- Continuity: The construction of the continuity equation is founded on the principle of mass conservation, and it is expressed in a general form as follows:

$$\frac{\partial U_i}{\partial x_i} = 0. \qquad (1)$$

- Momentum: The formulation of the momentum equation is grounded in the principle of momentum conservation, in accordance with Newton's second law, and being succinctly expressed as follows:

$$\frac{\partial U_i}{\partial t} + \frac{\partial U_j U_i}{\partial x_j} = \frac{\partial}{\partial x_j}\left(\mu \frac{\partial U_i}{\partial x_j}\right) - \left(\frac{\partial}{\partial x_j}\left(\overline{u_i u_j}\right) + \frac{1}{\rho}\frac{\partial p}{\partial x_j}\right), \qquad (2)$$

Where, ρ signifies the density of fluid, U_i represents the mean velocity vector, μ stands for dynamic viscosity, and p

denotes the static pressure. In turbulent flow scenarios, the time-averaging procedure produces the unspecified Reynolds stresses ($u_i u_j$), necessitating their modelling through turbulence theory. Conversely, in laminar flows, the Reynolds stresses decrease substantially towards zero. Arterial stenosis of moderate to severe degree has the potential to create significantly disrupted flow patterns downstream of the stenosis site, featuring turbulent flow patterns. The viscosity of blood flow is determined using the Carreaumodel **[24]**:

$$\mu(\dot{\gamma}) = \mu_\infty + (\mu_0 - \mu_\infty)[1 + (\lambda\dot{\gamma})^2]^{\frac{n-1}{2}}, \quad (3)$$

Where λ stands for the relaxation time (λ = 3.313 s), n = 3.568, μ_∞ = 3.5 × 10^−3 Pa s, and μ_0 = 5.6 × 10^−2 Pa s.

Given the limitations of laminar flow modelling and Reynolds Averaged Navier-Stokes(RANS) based turbulence models in accurately representing fully turbulent flows **[25]**, this study employs the transitional Shear Stress Transport (SST) k-ω model **[26]**. Specifically designed to detect transitions to turbulent states, the SST k-ω model includes additional equations for intermittency and criteria for transition onset. Additional elaboration on this model, with justification for its application under physiological flow conditions was reported by **[17,27,28]**.

$$\rho\left(\frac{\partial}{\partial x_i}(ku_i) + \frac{\partial}{\partial t}(k)\right) = \frac{\partial}{\partial x_j}\left(\Gamma_k \frac{\partial k}{\partial x_j}\right) + Y_k + G_k, \quad (4)$$

$$\rho\left(\frac{\partial}{\partial x_i}(\omega u_i) + \frac{\partial}{\partial t}(\omega)\right) = \frac{\partial}{\partial x_j}\left(\Gamma_\omega \frac{\partial \omega}{\partial x_j}\right) + D_\omega + Y_\omega + G_\omega. \quad (5)$$

Here, Y denotes the diffusion term, Γ denotes effective diffusivity, G stands for the generation term and D denotes cross-diffusion.

Boundary conditions

In the domain of fluid, the inlet is positioned at the CCA and is configured to feature blood flow pulsatile profile, similar to that used in Ref. [17]. Three distinct time steps are utilised to illustrate the results, involving systolic phase at t= 0.2 s, early diastole phase at t= 0.3 s and late diastole phase at t= 0.7s. The simulations are conducted over three cardiac cycles. Transient pressure waveforms are applied as boundary conditions at the outlets, similar to that employed in Ref. [17], with peak pressure happening at t = 0.45 s, highlighting the temporal offset between peak flow and pressure levels during the cardiac cycle.

Results and Discussion

The influence of WSS on blood flow along the vessel wall has been demonstrated to significantly affect the evolution of atherosclerotic plaque from initiation to progression and eventual destabilisation. Increased changes in shear stress within plaques-containing regions coincide with lumen constriction and increased vulnerability of lesions [29,30]. It was indicated by other researchers [31] that high shear stress correlates with fibrous cap degradation in stenotic lesions and the development of a plaque phenotype prone to rupture. **Figure 2a-2c** depict WSS gradients during both systolic and diastolic phases within the plaques and carotid web regions. At systolic phase, a significant increase of WSS is mainly found at plaque locations and the region of carotid web. Elevated shear stress within the lesion's neck region can further facilitate pathophysiological processes that destabilise the plaque and thicken the fibrous cap, ultimately culminating in plaque disruption. On the contrary, in diastolic phase, when WSS levels decrease, there is an increased tendency for plaque progression and arterial remodelling characterised by constriction.

It is seen in **Figure 2d** that WSS shows a significant increased values at stenosed regions, particularly at web and apex plaque regions. Furthermore, the plaque located at inner posterior wall of the ICA sinus experienced exceptionally low WSS, with the minimum value observed at the proximal end of the ICA bulb (following the web region), whereas WSS levels were notably elevated downstream of the ICA. This region may display an increased susceptibility to plaque development. In conducted studies by other researchers [32], it was observed that secondary turbulence, low WSS, and recirculating flows downstream from the stenosis are typical characteristics associated with disease progression. Usually, lesions evolve at low shear stress [33,34]. The region downstream of the carotid plaque, subjected to low and oscillatory shear stress, exhibits a notably higher concentration of vascular smooth muscle cells and reduced inflammation. Conversely, the upstream shoulder region, potentially exposed to low shear stress, displays increased inflammation, characterised by significant presence of macrophages and elevated gelatinolytic activity [35]. WSS exerted on the endothelial cells that line the inner surface of blood vessels serves as mechanical stimuli, initiating biological signalling pathways essential for maintaining vascular homeostasis [36]. Prolonged deviations of WSS from physiological norms lead to a variety of endothelial cell-mediated mechanisms, such as vascular remodelling, extracellular matrix degradation, cellular apoptosis, and proinflammatory reactions [34]. The findings of this study validate earlier studies indicating that lower values of WSS, reduced velocity magnitudes, and vortex distribution downstream contribute to plaque formation on the distal side. Diminished WSS magnitudes impact cellular flow rate, resulting in a notable augmentation of cell movement and increased disruption in intracellular connections. This subsequently leads to intensified LDL permeability of arterial walls [37].

Hence, when a stenosis arises in the artery (at the carotid bifurcation or following carotid web induced highly disturbed flow), the growth rate of plaques increase, and the likelihood of the formation of new plaque is amplified within the post-stenotic region of the stenosis, particularly in the zone of flow reattachment. The outcome concurs with the experimental observations of Deng et al. [30], who observed increased cholesterol uptake within the region of reattachment.

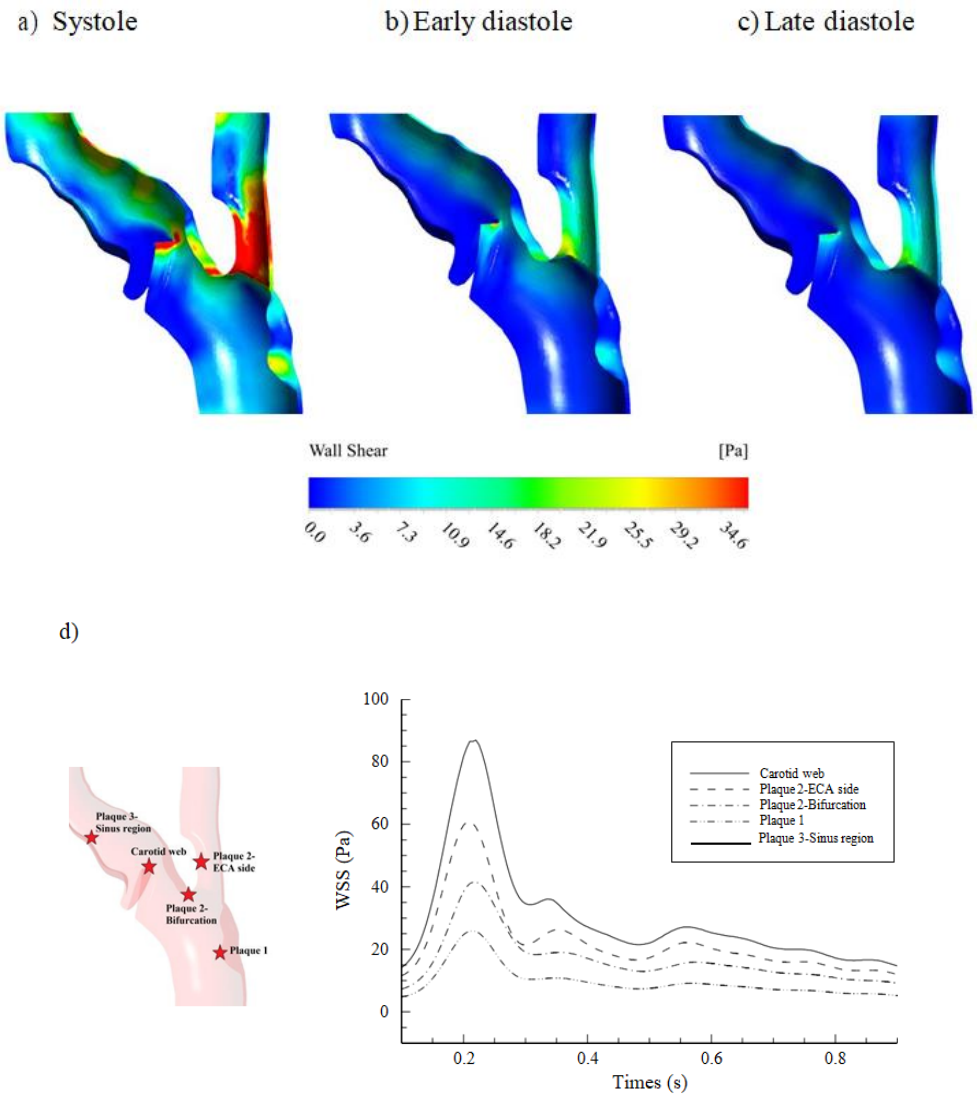

Figure 2: WSS gradients for the region of plaques and carotid web at different time instants, a) Systole, b) Early diastole, c) Late diastole; d) WSS variation at different locations over the cardiac cycle.

The flow patterns within the carotid artery were depicted using instantaneous streamlines and velocity contour plots, with colours representing blood flow velocity magnitude at various time intervals **(Figure 3a-3c)**. A thorough examination of the computational findings reveals the typical features observed in the carotid sinus, including the occurrence of reverse axial flow during the peak of systole, persisting until the conclusion of diastole, primarily attributable to the existence of the carotid web. The blood flow within constricted regions affected by stenosis exhibited notably greater velocity compared to that in the CCA and upstream of the bifurcation, maintaining a skewed trajectory following the stenosis. On the contrary, the blood flow velocity within the ICA bulb region was observed to be lower compared to other regions of the artery. This phenomenon, particularly evident near the proximal aspect of the carotid web, indicates consistently disturbed flow dynamics across all time intervals. The distribution of velocity across various points during the cardiac cycle, as depicted in **Figure 4**, illustrates that the highest velocity is observed in proximity to the stenosis of the ECA and the lesion connected to carotid apex, with similar values detected downstream of the ECA. Conversely, the CCA exhibits the lowest velocity magnitude, attributable to its larger arterial diameter in that particular segment.

a) Velocity streamline and the contours of velocity module at different planes in systolic phase

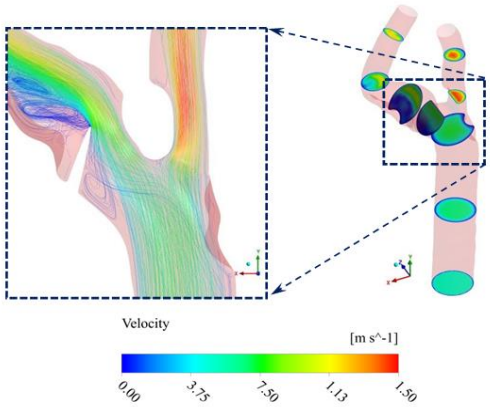

b) Velocity streamline and the contours of velocity module at different planes in early diastolic phase

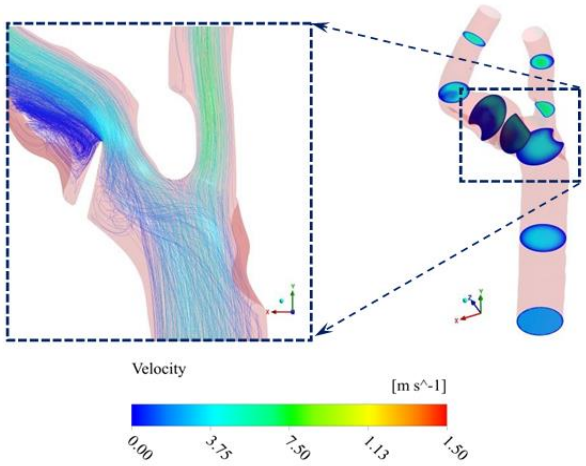

c) Velocity streamline and the contours of velocity module at different planes in latediastolic phase

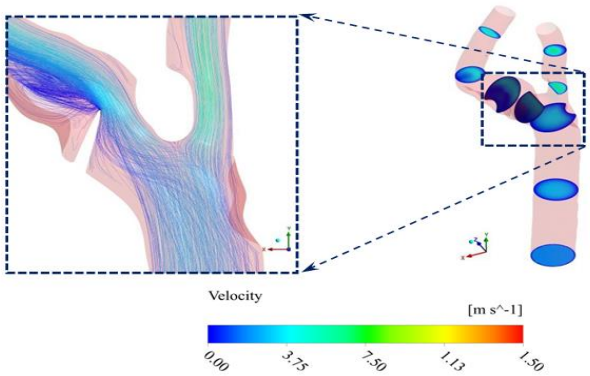

Figure 3: Velocity streamlines and the contours of velocity module at a) Systolic phase, b)Early diastolic phase, c) End diastolic phase.

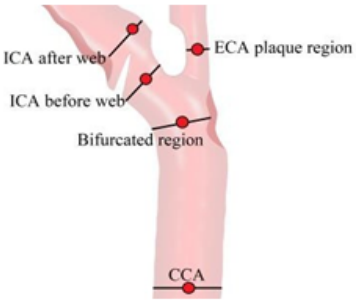

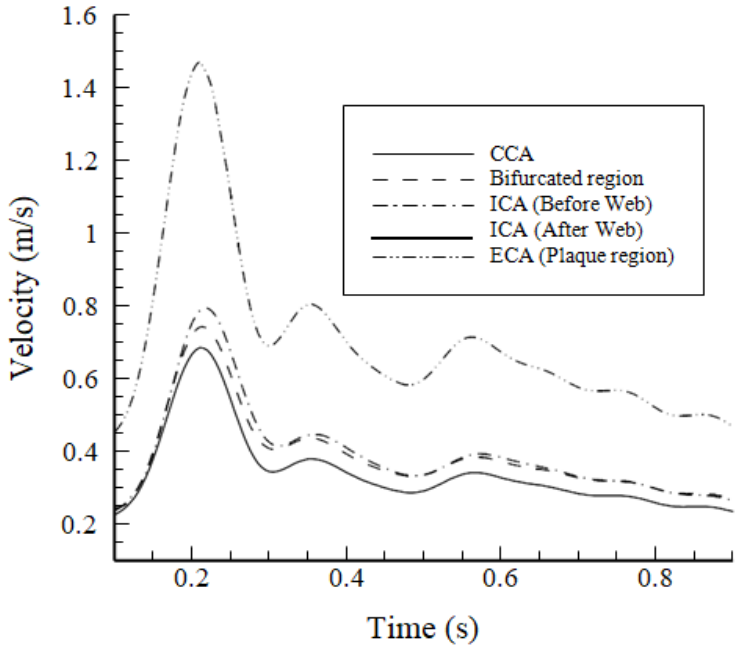

Figure 4: Velocity variations at different locations.

Conclusion

A CFD model of a diseased carotid artery comprising plaques and carotid web has been presented in this paper using a patient specific geometry. The geometry of a moderate stenosis plaque, along with a web characterised by an acute angle and length, were simulated to determine the critical condition of the carotid artery. Variation of hemodynamic simulations parameters, i.e. velocity and WSS, has been investigated. Through the study presented in the paper, the following conclusions can be drawn:

- The simulation results show there was a swirling or disturbed systolic flow existing in the region affected by the web and proximal to the bifurcation.
- These conditions may predispose the plaque to rupture and cause damage to the downstream wall.
- A variety of flow disruptions were noted in the vicinity of the stenosis area, which might result in the elevated shear stress in the region of the plaques and reduced shear stress in the area following the plaques.

Acknowledgement

The support from the University of Adelaide, School of Electrical and Mechanical Engineering and Department of Education, Skills and Employment Research Training Program (RTP) scholarship, is acknowledged.

References

1. Namaganda P, J Nakibuuka, M Kaddumukasa, E Katabira. Stroke in young adults, stroke types and risk factors: a case control study. BMC Neurol. 2022;22(1):335.
2. Li, X., H.-M. Wang, C.-H. Xiang, Z.-S. Li, J.-H. Zhao, X.-M. Zhang, J. Jiao, J. Liu, Q. Wang, Q. Song. From Near Death to Recovery in Exertional Heat Stroke: Lessons Learned from a Long Distance Runner's Case. Mega J Case Rep. 2024;7(3):2001-2010.
3. Benjamin, E. J., S. S. Virani, C. W. Callaway, A. M. Chamberlain, A. R. Chang, S. Cheng, S. E. Chiuve, M.

Cushman, F. N. Delling, R. Deo. Heart disease and stroke statistics—2018 update: a report from the American Heart Association. 2018;137(12):e67-e492.

4. Ahmadpour-B, M., A. Nooraeen, M. Tafazzoli-Shadpour, H. Taghizadeh. Contribution of atherosclerotic plaque location and severity to the near-wall hemodynamics of the carotid bifurcation: an experimental study and FSI modeling. Biomech Model Mechanobiol. 2021;20(3):1069-1085.
5. Younis, H., M. Kaazempur-Mofrad, C. Chung, R. Chan, R. Kamm. Computational analysis of the effects of exercise on hemodynamics in the carotid bifurcation. Ann Biomed Eng. 2003;31(8):995-1006.
6. Multon, S., C. Denier, P. Charbonneau, M. Sarov, D. Boulate, D. Mitilian, J. Mougin, O. Chassin, N. Legris, E. Fadel. Carotid webs management in symptomatic patients. J Vasc Surg. 2021;73(4):1290-1297.
7. Boesen, M. E., P. V. Eswaradass, D. Singh, A. P. Mitha, M. Goyal, R. Frayne, B. K. Menon. MR imaging of carotid webs. Neuroradiology. 2017;59(4):361-365.
8. Haussen, D. C., J. A. Grossberg, M. Bouslama, G. Pradilla, S. Belagaje, N. Bianchi, J. W. Allen, M. Frankel, R. G. Nogueira. Carotid web (intimal fibromuscular dysplasia) has high stroke recurrence risk and is amenable to stenting. Stroke. 2017;48(11):3134-3137.
9. Ning, B., D. Zhang, B. Sui, W. He. Ultrasound imaging of carotid web with atherosclerosis plaque: a case report. J Med Case Rep. 2020;14(1):145.
10. Ben, Z., J. Wang, J. Zhan, S. Chen. Ultrasonic characteristics of carotid webs. Neuroradiology. 2022;64(1):95-98.
11. Kumar, N., A. Khader, R. Pai, P. Kyriacou, S. Khan, P. Koteshwara. Computational fluid dynamic study on effect of Carreau-Yasuda and Newtonian blood viscosity models on hemodynamic parameters. J Computational Methods Sci Eng. 2019;19:465-477.
12. Lee, S. H., K.-S. Han, N. Hur, Y. I. Cho, S.-K. Jeong, The effect of patient-specific non-Newtonian blood viscosity on arterial hemodynamics predictions. J Mechanics Med Biol. 2019;19:1940054.
13. Li, C.-H., B.-L. Gao, J.-W. Wang, J.-F. Liu, H. Li, S.-T. Yang. Hemodynamic factors affecting carotid sinus atherosclerotic stenosis. World Neurosurg. 2019:121:e262-e276.
14. Kanokjaruvijit, K., T. Donprai-On, N. Phanthura, P. Noidet, J. Siripokharattana. Wall shear stress and velocity distributions in different types of stenotic bifurcations. J Mech Sci Tech. 2017;31:2339-2349.
15. Movahed, M. R., Coronary artery bifurcation lesion classifications, interventional techniques and clinical outcome. Expert Rev Cardiovasc Ther. 2008;6(2):261-74.
16. Sousa, L. C., C. F. Castro, C. C. António, F. Sousa, R. Santos, P. Castro, E. Azevedo. Computational simulation of carotid stenosis and flow dynamics based on patient ultrasound data–A new tool for risk assessment and surgical planning. Adv Med Sci. 2016;61(1):32-9.
17. Moghadasi, K., M. H. Ghayesh, E. Hu, J. Li, Nonlinear biomechanics of diseased carotid arteries. Int J Eng Sci. 2024;199:104070.
18. MATLAB simulink, (R2021b).
19. ANSYS Fluent 2023 R1. 2023.
20. Noh, S.-M., H. G. Kang, Clinical significance of the internal carotid artery angle in ischemic stroke. Sci Rep. 2019;9(1):4618.
21. Qian, H., L. Wang, Practical Techniques of Carotid Endarterectomy. Springer. 2023.
22. Serrin, J., Mathematical principles of classical fluid mechanics, in: Fluid Dynamics I/Strömungsmechanik I, Springer. 1959;125-263.
23. Chorin, A. J., J. E. Marsden, J. E. Marsden, A mathematical introduction to fluid mechanics. Springer. 1990.
24. Lopes, D., H. Puga, J. Teixeira, S. Teixeira. Fluid–Structure Interaction study of carotid blood flow: Comparison between viscosity models. Eur J Mechanics-B/Fluids. 2020;83:226- 234.

25. Arun, M., E. Tulapurkara, Computation of turbulent flow inside an enclosure with central partition, Progress in Computational Fluid Dynamics Int J. 2005;5:455-465.
26. Mahalingam, A., U. U. Gawandalkar, G. Kini, A. Buradi, T. Araki, N. Ikeda, A. Nicolaides, J. R. Laird, L. Saba, J. S. Suri. Numerical analysis of the effect of turbulence transition on the hemodynamic parameters in human coronary arteries. Cardiovasc Diagn Ther. 2016;6(3):208-20.
27. Carpenter, H. J., A. Gholipour, M. H. Ghayesh, A. C. Zander, P. J. Psaltis, In Vivo Based Fluid– Structure Interaction Biomechanics of the Left Anterior Descending Coronary Artery. J Biomech Eng. 2021;143(8):081001.
28. Carpenter, H. J., M. H. Ghayesh, A. C. Zander, P. J. Psaltis. On the nonlinear relationship between wall shear stress topology and multi-directionality in coronary atherosclerosis. Comput Methods Programs Biomed. 2023:231:107418.
29. Gijsen, F., F. Mastik, J. A. Schaar, J. Schuurbiers, W. J. van der Giessen, P. J. de Feyter, P. W. Serruys, A. Van Der Steen, J. J. Wentzel, High shear stress induces a strain increase in human coronary plaques over a 6-month period. EuroIntervention. 2011;7(1):121-7.
30. Malik, J., L. Novakova, A. Valerianova, E. Chytilova, V. Lejsek, K. Buryskova Salajova, L. Lambert, T. Grus, M. Porizka, P. Michalek, Wall shear stress alteration: a local risk factor of atherosclerosis. Curr Atheroscler Rep. 2022;24(3):143-151.
31. Samady, H., P. Eshtehardi, M. C. McDaniel, J. Suo, S. S. Dhawan, C. Maynard, L. H. Timmins, A. Quyyumi, D. P. Giddens, Coronary artery wall shear stress is associated with progression and transformation of atherosclerotic plaque and arterial remodeling in patients with coronary artery disease. Circulation. 2011;124(7):779-88.
32. Birchall, D., A. Zaman, J. Hacker, G. Davies, D. Mendelow, Analysis of haemodynamic disturbance in the atherosclerotic carotid artery using computational fluid dynamics. Eur Radiol. 2006;16(5):1074-83.
33. Moerman, A., S. Korteland, K. Dilba, K. van Gaalen, D. Poot, A. van Der Lugt, H. Verhagen, J. Wentzel, A. van Der Steen, F. Gijsen, The correlation between wall shear stress and plaque composition in advanced human carotid atherosclerosis. Front Bioeng Biotechnol. 2022:9:828577.
34. Szajer, J., K. Ho-Shon. A comparison of 4D flow MRI-derived wall shear stress with computational fluid dynamics methods for intracranial aneurysms and carotid bifurcations—a review. Magn Reson Imaging. 2018:48:62-69.
35. Moerman, A., S. Korteland, K. Dilba, K. van Gaalen, D. Poot, A. van Der Lugt, H. Verhagen, J. Wentzel, A. van Der Steen, F. Gijsen, The correlation between wall shear stress and plaque composition in advanced human carotid atherosclerosis. Front Bioeng Biotechnol. 2022:9:828577.
36. Nixon, A. M., M. Gunel, B. E. Sumpio, The critical role of hemodynamics in the development of cerebral vascular disease: a review. J Neurosurg. 2010;112(6):1240-53.
37. Kadohama, T., K. Nishimura, Y. Hoshino, T. Sasajima, B. E. Sumpio, Effects of different types of fluid shear stress on endothelial cell proliferation and survival. J Cell Physiol. 2007;212(1):244-51.

Citation of this Article

Moghadasi K, Ghayesh MH, Hu E and Li J. Coupled Effect of the Presence of Plaque and Carotid Web for the Assessment of hemodynamic parameters in a Patient Carotid Artery: A CFD Study. Mega J Case Rep. 2024;7(5):2001-2011.

Copyright